Supporting Information for:

On the Mechanism of the Quorum-Quenching Lactonase (AiiA) from Bacillus thuringiensis: 2. Substrate Modeling and Active Site Mutations

Jessica Momb, Canhui Wang, Dali Liu, Pei W. Thomas, Gregory A. Petsko, Hua Guo, Dagmar Ringe and Walter Fast

1. Steady-state kinetic studies:

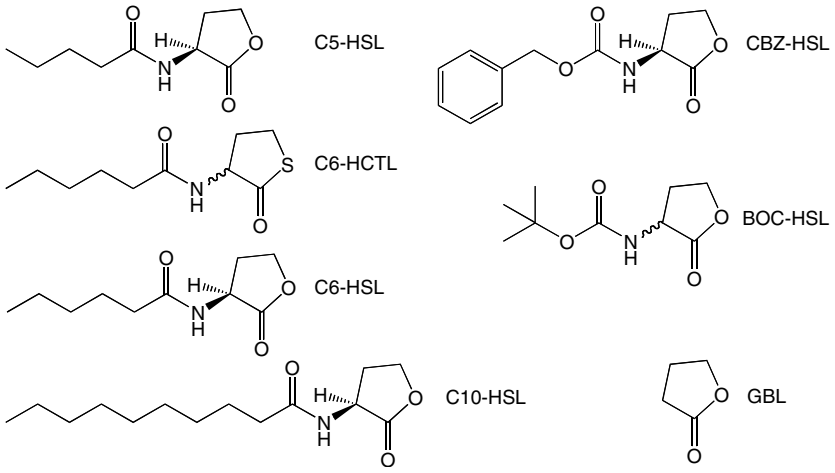

Supplemental Figure S1. Structures of Substrates Used In Kinetic Studies. Abbreviations are defined in Materials and Methods.

2. Circular Dichroism Spectroscopy of AHL Lactonase:

Far UV-circular dichroism spectra of wild type and mutant dicobalt AHL lactonases were compared to assess changes in secondary structure upon mutation. Briefly, proteins were transferred into sodium phosphate buffer (10 mM) , pH 7.4 by buffer exchange (Amicon Ultra-4 10,000 kDa MWCO, Millipore), and made to final concentrations of 45-95 µg / mL using the same buffer, as determined by the BCA protein assay kit (Pierce). Sodium phosphate buffer (10 mM), pH 7.4 was used as the baseline buffer used for all samples. CD spectra (190 – 240 nm, with a wavelength step

of 0.1 nm) were obtained using five scans on a JASCO J-810 spectropolarimeter operating at room temperature. Ellipticity values at each wavelength for all five scans were averaged, and these averages were used in further analysis. Elliptical rotation was converted to molar ellipticity [θ], and is plotted versus wavelength for each protein sample analyzed in Figure S2.

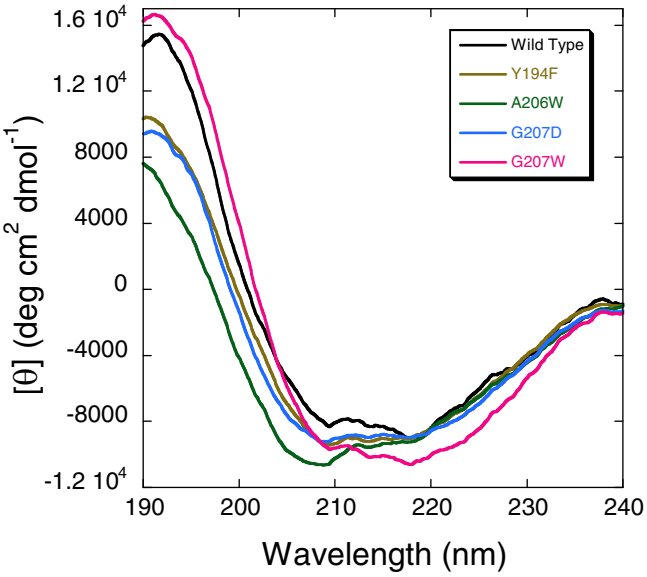

Supplemental Figure S2. CD Spectra of Dicobalt AHL Lactonase Variants. Five spectra are overlain to visualize difference in far UV molar ellipticity between AHL lactonase variants, wild-type (black), Y194F (gold), A206W (green), G207D (blue), and G207W (pink).

The CD spectra were analyzed for secondary structural content using the SELCON3 simulation program and data set SP175(*1*) available at DICHROWEB (http://www.cryst.bbk.ac.uk/cdweb/html/home.html) (*2, 3*). Predicted alpha helix and beta sheet content are presented in Table S1. The generally accepted interpretation of normalized standard deviation (NRMSD) for CD data is that an NRMSD of less than 0.2

indicates the calculated structure is generally similar to the actual structure (*4*), and the values obtained here are within this cutoff. Indeed, the alpha and beta character of all samples are similar to those calculated for the crystal structure of dizinc AHL lactonase (*5*). The D108N mutant AHL lactonase is purified as a fusion protein that lacks a TEV protease cleavage site, and so is not included in this comparison.

Table S2. Calculated Secondary Structure Content of AHL Lactonase Variants

	α-helix (%)	β-sheet (%)	Turns (%)	Unordered (%)	NRMSD
Wild Type	18	33	12	37	0.10
Y194F	18	33	11	37	0.09
A206W	22	28	10	38	0.19
G207D	19	29	11	37	0.11
G207W	23	29	10	37	0.07
calculated[a]	25	30	-[b]	-	-

[a] From PDB ID 2A7M (*6*)
[b] Not calculated

There are slight differences in predicted α-helix and β-sheet content between wild-type and mutant enzymes, with the Y194F mutant having the greatest similarity to the wild type enzyme and the Gly to Trp mutations (A206W and G207W) having the largest. The negative bands at 222 and 208 nm corresponding to α-helical character (*7*) overlap quite well, while more deviation is seen in the positive band near 198 nm corresponding to a portion of the β-sheet region (*7*). It is known that more strongly twisted β-sheets have a stronger 198 nm band (*7*). It is possible that the Y194F, G207D and A206W mutations cause slight changes in conformation that relax one or more strongly twisted β-sheets; these residues are adjacent to ends of the β10-12 strands. These mutations might instead cause a more global change in conformation. However,

they appear to have little impact at the active site of the enzyme. For example, the mutant with the largest change in predicted secondary structure, A206W, still binds two equivalents of metal ion and has a k_{cat}/K_M value for the unsubstituted GBL substrate that is only 15% different than that of wild type enzyme. Therefore, functional changes that arise from the mutations described herein, most likely derive from local changes in conformation. Of course, more detailed structural studies will be required to characterize the exact nature of these changes.

3. Supplemental References

(1) Lees, J. G., Miles, A. J., Wien, F., and Wallace, B. A. (2006) A reference database for circular dichroism spectroscopy covering fold and secondary structure space. *Bioinformatics 22*, 1955-1962.

(2) Whitmore, L., and Wallace, B. A. (2004) DICHROWEB, an online server for protein secondary structure analyses from circular dichroism spectroscopic data. *Nucleic Acids Res. 32*, W668-W673.

(3) Whitmore, L., and Wallace, B. A. (2008) Protein secondary structure analyses from circular dichroism spectroscopy: Methods and reference databases. *Biopolymers 89*, 392-400.

(4) Mao, D., Wachter, E., and Wallace, B. A. (1982) Folding of the mitochondrial proton adenosinetriphosphatase proteolipid channel in phospholipid vesicles. *Biochemistry 21*, 4960-4968.

(5) Liu, D., Lepore, B. W., Petsko, G. A., Thomas, P. W., Stone, E. M., Fast, W., and Ringe, D. (2005) Three-dimensional structure of the quorum-quenching *N*-acyl

homoserine lactone hydrolase from *Bacillus thuringiensis*. *Proc. Natl. Acad. Sci. USA 102*, 11882-11887.

(6) Kabsch, W., and Sander, C. (1983) Dictionary of protein secondary structure: pattern recognition of hydrogen-bonded and geometrical features. *Biopolymers 22*, 2577-2637.

(7) Sreerama, N., and Woody, R. W. (2004) Computation and analysis of protein circular dichroism spectra. *Methods Enzymol. 383*, 318-351.